

Protein crystallography beamline (PX-BL21) at Indus-2 synchrotron

Ashwani Kumar,^a Biplab Ghosh,^a H. K. Poswal,^a K. K. Pandey,^a Jagannath,^b M. V. Hosur,^c Abhilash Dwivedi,^a Ravindra D. Makde^a and Surinder M. Sharma^{a*}

^aHigh Pressure and Synchrotron Radiation Physics Division, Bhabha Atomic Research Center, Trombay, Mumbai, India,

^bTechnical Physics Division, Bhabha Atomic Research Center, Trombay, Mumbai, India, and ^cAdvanced Centre for Treatment, Research and Education in Cancer, Navi Mumbai, India. *Correspondence e-mail: smsharma@barc.gov.in

Received 8 October 2015

Accepted 14 January 2016

Edited by J. F. van der Veen

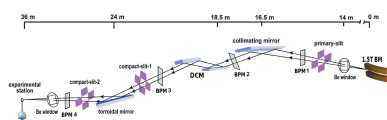
Keywords: protein crystallography; beamline; bending magnet; Indus-2.

The protein crystallography beamline (PX-BL21), installed at the 1.5 T bending-magnet port at the Indian synchrotron (Indus-2), is now available to users. The beamline can be used for X-ray diffraction measurements on a single crystal of macromolecules such as proteins, nucleic acids and their complexes. PX-BL21 has a working energy range of 5–20 keV for accessing the absorption edges of heavy elements commonly used for phasing. A double-crystal monochromator [Si(111) and Si(220)] and a pair of rhodium-coated X-ray mirrors are used for beam monochromatization and manipulation, respectively. This beamline is equipped with a single-axis goniometer, Rayonix MX225 CCD detector, fluorescence detector, cryogenic sample cooler and automated sample changer. Additional user facilities include a workstation for on-site data processing and a biochemistry laboratory for sample preparation. In this article the beamline, other facilities and some recent scientific results are briefly described.

1. Introduction

The number of protein structures deposited in the Protein Data Bank (PDB) (Berman *et al.*, 2003) has increased exponentially over the last decade. The availability of protein crystallography beamlines on synchrotron rings around the world has been largely responsible for this phenomenon. The high brilliance of X-ray beams delivered on the sample crystals has enabled scientists to collect accurate diffraction data from crystals with small diffracting power. The energy tunability of the X-ray beams has enabled scientists to exploit the phenomenon of anomalous diffraction to speedily solve the crystallographic ‘phase problem’. The quality of diffraction data collected on a synchrotron source is generally also so much better than that obtainable on a home source, due to high brilliance, energy tunability and cutting-edge instrumentation with better computing resources, such that a synchrotron source is preferable for quality data collection. In this context it is significant that a protein crystallography beamline has been made operational on the Indus-2 synchrotron in India.

The Indus-2 synchrotron is an electron storage ring (Ghodke *et al.*, 2006) designed for 2–2.5 GeV beam energy and stored current up to 200 mA (Ghodke & Hannurkar, 2014) at Raja Ramanna Center for Advanced Technology (RRCAT), Indore, India. The synchrotron has been in regular operation at 2.5 GeV beam energy with ~150 mA of stored beam current; it is operated in decay mode with a typical lifetime of ~22 h at 100 mA of stored beam current (Kumar *et al.*, 2013). The storage ring operates with horizontal and



vertical beam emittance of 58 nmrad and 0.58 nmrad, respectively. Recently, Indus-2 has been upgraded to a third-generation source with the commissioning of two undulators (Hannurkar, 2015). The protein crystallography beamline (PX-BL21) is a newly constructed bending-magnet beamline on Indus-2 with a working energy range of 5–20 keV. However, in the future, the beamline will be shifted to a 2.5 T superconducting multipole wiggler port which will require some of the beamline components to be upgraded to take care of higher thermal loads from the multipole wiggler. There is also an ancillary biochemistry laboratory associated with this beamline to facilitate the beamline users at various stages of crystal preparation and optimization. This beamline is a national facility and the Department of Atomic Energy (DAE), Government of India, has funded its construction and operation. PX-BL21 is primarily aimed to cater for the needs of more than 100 independent research groups in India working in the area of structural biology. The first diffraction data on single crystals of the lysozyme protein were recorded during mid-2012 and since then the beamline has been used by several users (Goyal *et al.*, 2014; Arif *et al.*, 2015; Sonani *et al.*, 2015; Agarwal *et al.*, 2015).

2. Beamline overview

2.1. Photon source and the front-end

The photon source for this beamline is a 1.5 T bending magnet located at port No. 21 (5° port) of the Indus-2 synchrotron. The beamline front-end (FE) (Raghuvanshi *et al.*, 2007), which finishes at 14 m from the source, has most of its components inside the thick concrete wall of the Indus-2 ring. The FE consists of a fixed-exit copper mask that provides 2.2 mrad horizontal aperture, and allows full vertical size for the white beam. The FE also contains various pneumatic gate valves, water-cooled shutters including the safety shutter and the fast-closing shutter. The FE makes use of the fast-closing shutter and a delay line for ultrahigh-vacuum (UHV) protection of the storage ring. The 250 μm-thick beryllium window at the end of the FE separates the storage ring vacuum from that of the beamline. It also acts as a high-pass filter removing photons with energy below ~5 keV, thus

reducing the heat load on the downstream optical components.

2.2. Beamline optics

The beamline is 36 m long starting from the source to the sample position and is operated under UHV (~10⁻⁸ mbar). It comprises several components, namely primary slit, two compact slits, collimating mirror (CM), four wire-cum-fluorescence beam-position monitors (BPMs), double-crystal monochromator (DCM), focusing toroidal mirror (TM) and an experimental station as depicted schematically in Fig. 1. All these components are water-cooled (297 ± 0.5 K), except the experimental station. Lead-shielded hutches and interlocked doors are provided to protect users from ionizing radiation.

The primary slit is placed just after the FE to select the central cone of the X-ray beam for the CM, with optimal dimension. The profile and the position of the X-ray beam after the primary slit is measured by BPM-1. All BPMs are equipped with a phosphor-coated water-cooled copper block with an electrically isolated tungsten wire attached at its bottom. The vertical beam profile, measured from the photocurrent, is generated by scanning the tungsten wire through the X-ray beam. The white X-ray beam shines at an incident angle of 3 mrad on the flat surface of a dynamically bendable CM reflecting it downward. The CM is a rhodium-coated 1.2 m long single piece of silicon crystal, which ensures a flat reflectivity response for the X-rays in the working energy range of the beamline. The CM improves the energy resolution by collimating the X-ray beam in the vertical plane. BPM-2, installed immediately after the CM, is used for the in-beam alignment of the latter. The DCM is installed at 18.5 m from the source and provides a tunable monochromatic X-ray beam with energy in the range 5–20 keV. The DCM uses a pair of flat Si crystals in (+, -) configuration, which ensures constant exit beam height and angle. The DCM consists of two pairs of crystals, Si(111) and Si(220), which can be exchanged in-vacuum as per the user requirement for resolution. The second crystal of the DCM is fitted with a piezoelectric actuator that is used for continuous and automatic beam stabilization through a feedback control system called MOSTAB (monochromator stabilizer) (Krolzig *et al.*, 1984). The monochromatic beam can be resized by using the compact slit downstream of the DCM,

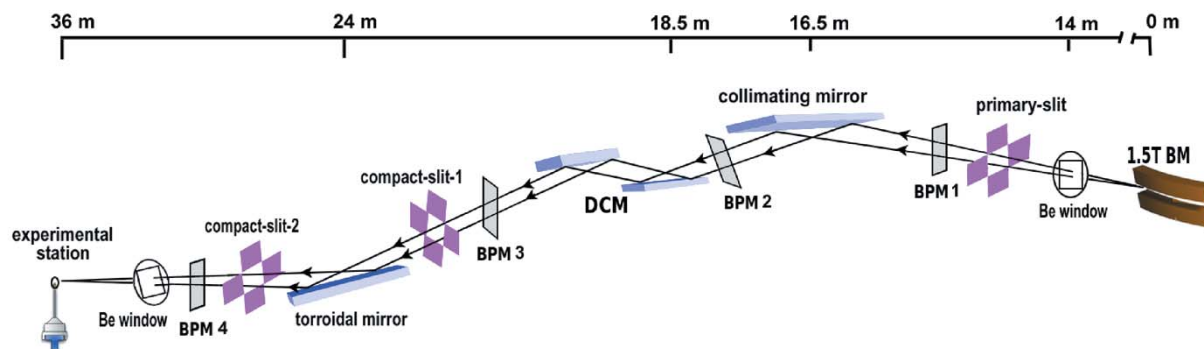


Figure 1

Schematic of PX-BL21 showing various optical and diagnostic components: slits, collimating mirror, toroidal mirror, double-crystal monochromator (DCM), beam-position monitors *etc.*

while BPM-3 helps the alignment of the DCM in the X-ray beam.

Finally the monochromatic beam is focused in both the vertical and the sagittal planes on the sample by using the TM placed at 24 m from the source. The TM is also a 1.2 m long rhodium-coated silicon mirror with fixed sagittal radius (48.5 mm) and variable tangential curvature. The toroidal mirror is used in 2:1 configuration (MacDowell *et al.*, 2004), as this configuration along with the vertical pre-collimation of the X-ray beam can provide a better image quality by minimizing the comatic aberrations (sagittal and tangential). Both mirrors are placed on hexapods (Stewart, 1965), which provide a rigid and vibration-free support to the X-ray mirrors and allow precise movements with $\sim 10 \mu\text{m}$ (translational) and $\sim 0.1 \text{ mrad}$ (angular) accuracies.

The beamline components, such as the primary slit, compact slits, mirror chambers along with hexapods, beam pipes, support tables and BPMs, were designed and developed indigenously. The CM and TM including the benders and the cooling systems were built by SESO, France, while the DCM was supplied by FMB Berlin, Germany.

2.3. Experimental station

The monochromatic X-ray beam finally comes out into air through a beryllium window, upstream of the experimental station. A foil holder along with the ionization chamber is placed between the beryllium window and the experimental station, for the calibration of the DCM through measurement of the absorption energy of the elements in the foil. The experimental station (Fig. 2) of the beamline is equipped with a (i) single-axis goniometer system (mardtb, Marresearch, Germany) with dedicated real-time operating system and network interface to the host computer, (ii) MX225 CCD (Rayonix USA) detector, (iii) fully automatic cryogenic sample changer (marcsc, Marresearch, Germany), (iv) cryostream system (Oxford 700 series) and (v) XR-100SDD silicon drift detector (AMPTEK). The collimator of the mardtb system has two ionization chambers and two pairs of motor-

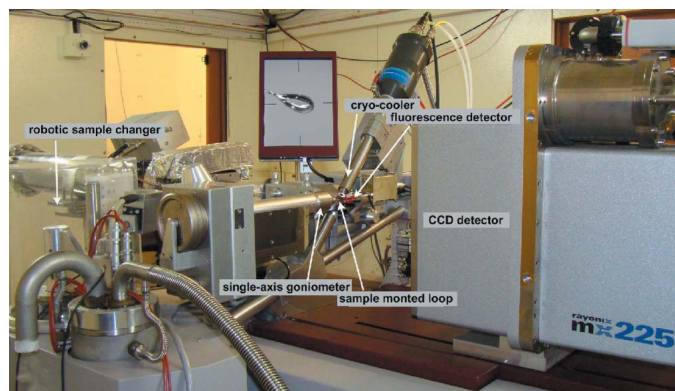


Figure 2
Experimental station at PX-BL21 showing the CCD detector, sample cooler, fluorescence detector, single-axis goniometer and robotic sample changer.

Table 1
Beamline details.

Beamline name	PX-BL21
Source type	1.5 T bending magnet
Mirrors	Both CM and TM are 1.2 m single-crystal Si with Rh coating
Monochromator	Water-cooled DCM with Si(111) and Si(220) crystals
Energy range (keV)	5–20
Wavelength range (Å)	0.62–2.48
Beam size (μm) (FWHM)	500×500
Flux (photons s^{-1}) [†]	1.2×10^{10}
Goniometer	Single-axis mardtb
Cryo capability	Liquid-nitrogen cryostream, 100–300 K
Sample mounting	marcsc automounter
Detector	Rayonix MX225 CCD
Detector angular displacement (2θ)	0–30°

[†] Measured using a calibrated AXUV 100 photodiode placed close to the sample position. The slit opening was $400 \mu\text{m} \times 400 \mu\text{m}$, X-ray energy was 12.658 keV, while the storage ring parameters were 2.5 GeV and $\sim 100 \text{ mA}$.

ized horizontal and vertical slits having aperture variable from 0 to 5 mm with resolution of $2.5 \mu\text{m}$. The dtb collimator is used for fully automatic search and intensity optimization of the X-ray beam. The single-axis goniometer of the dtb consists of a motorized high-precision φ -axis with a resolution of $0.0006^\circ \text{ step}^{-1}$.

The diffraction data are collected using the Rayonix MX225 detector coupled to the mardtb system. The sample-to-detector distance can be varied from a minimum of 75 mm to a maximum of 665 mm, *via* a motorized translational stage with a resolution of $1.25 \mu\text{m step}^{-1}$. The motorized vertical 2θ arm has a rotation range from 0° to 30° . SPINE standard sample holder and vials are compatible with the mardtb of this beamline. A storage dewar for 19 sample vials is attached to the mardtb system for fully automatic liquid sample transfer along with automatic refill system from self-pressurized liquid-nitrogen supply dewar. The Si-drift detector (SDD) is mounted on the mardtb, in an orthogonal direction to the X-ray beam, and in line with the goniometer axis, for fluorescence experiments and multiple wavelength anomalous diffraction (MAD) scans. The beamline parameters are summarized in Table 1.

2.4. Experiment control and data analysis

The beamline components are remotely controlled through their respective controllers and software. Microsoft Visual Basic (VB) has been used as the primary programming language for all of the optical components of the beamline other than the DCM. The DCM controller software has been supplied by FMB Oxford in VEE Pro (Agilent Technologies) language. The software for operating the hexapods and the slits was developed by the the Center for Design and Manufacture (CDM, BARC) while that for operating the BPMs was supplied by Excel Instruments Ltd (India). The experimental station is controlled by a dedicated Linux machine, and a single GUI (called marccd) for handling the mardtb, automatic beam alignment, CCD detector, manual/automatic crystal centering, data acquisition and marcsc sample changer

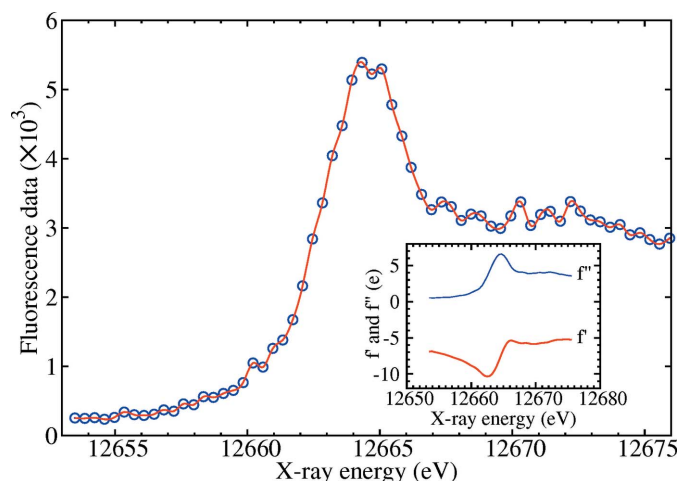


Figure 3 Experimental fluorescence spectrum from a selenomethionine protein measured at the Se *K*-edge. Inset: the anomalous scattering factors (f' and f'') are calculated from the experimental fluorescence data using the program *CHOOCH*. The value of f' at the peak (12664.70 eV) and the inflection (12662.46 eV) energies are -7.23 e and -10.35 e, respectively; while for f'' the respective values are 6.58 e and 3.49 e.

was supplied by Marresearch, Germany. The software for absorption-edge scanning using the SDD and DCM for anomalous diffraction experiments was developed by the authors. A fluorescence spectrum from a selenomethionine protein crystal measured at the Se *K*-edge using the energy tunability of the DCM and the absorption-edge scanning software is shown in Fig. 3. The calculated energy resolution from the fluorescence measurement is of the order of 10^{-4} with a Si(111) crystal. One can collect the diffraction data at both the peak and the inflection energies (see inset of Fig. 3) required for MAD experiments.

For on-site data analysis, a workstation with 12 Core Intel Xeon processor along with sufficient storage is available to users. The data analysis/processing software packages commonly used by protein crystallographers are also available, including *MOSFLM* (Leslie & Powell, 2007), *XDS* (Kabsch, 2010), *AUTOMAR* (Bartels & Klein, 2003), *CCP4* (Winn *et al.*, 2011), *SHELX* (Sheldrick, 2008), *PHENIX* (Adams *et al.*, 2010), *Pymol* (Schrödinger LLC, 2010) and *Chimera* (Pettersen *et al.*, 2004). Support related to the crystallization, data acquisition and data processing is provided to the users whenever required.

3. Ancillary facilities

An auxiliary biochemistry laboratory, adjacent to the beamline, has been set up for the PX-BL21 users for protein purifications and crystallizations. The laboratory is equipped with all the necessary instrumentation, which include a culture growth facility, centrifuges, protein purification systems, refrigerators (253 K and 193 K), stereozoom microscopes, constant temperature room (278–298 K), cold room (277 K) and liquid-nitrogen dewar for crystal storage. Further instrumentation, *e.g.* dynamic light scattering (DLS) system, circular

dichroism (CD) spectrometer and crystallization robot, will be made available to the users shortly.

4. Facility access

Facility access will be available through joint collaboration with the beamline scientists or by direct submission of experimental proposal through the online portal (<https://www.info-rrcat.ernet.in/beamline/>). Beam time is allotted after review of the proposal by a committee.

5. Highlights

Since commissioning, the PX-BL21 beamline is on regular operation and several research groups have collected data using this beamline. Until now, more than 100 datasets have been collected and about 15 structures have been deposited in the PDB. Our in-house research group has used the beamline and its ancillary facilities to determine structures using anomalous diffraction methods; some of these results are highlighted below.

5.1. SAD phasing of Xaa-Pro peptidases

The crystal structures of two Xaa-Pro peptidases (UniProt accession numbers Q9RUY4 and Q8P839) from *Deinococcus radiodurans* (XPDdr) and *Xanthomonas campestris* (XPDxc) have been determined using selenium and zinc single-wavelength anomalous diffraction (SAD) methods, respectively. These proteins are putative peptidases of the M24 metallo-peptidase family with bimetallic center in the active site. They specifically cleave the Xaa-Pro dipeptides that are resistant to cleavage by the other peptidases. In addition, these enzymes exhibit activity against toxic organophosphorus compounds such as pesticides and nerve agents. In bacteria, these enzymes are involved in the final degradation of the proline dipeptides and help in the recycling of proline. The Xaa-Pro dipeptidase activity of the enzymes is commercially important in the food and dairy industries for improving flavor and texture. We cloned, purified and crystallized the selenomethionine derivative of XPDdr (unpublished results) and XPDxc (Kumar *et al.*, 2014) proteins using the ancillary facilities of the beamline. To prepare the zinc derivative of XPDxc, the crystals were soaked for 24 h in mother liquor containing 1 mM $ZnCl_2$. The crystals were cryoprotected in the presence of 20% glycerol and frozen in liquid nitrogen. The diffraction data were recorded at 100 K and at the peak energies (where the imaginary component of the scattering factor, f'' , is maximum) of the selenium and zinc elements (12666 eV and 9669 eV, respectively). The data of XPDdr and XPDxc were collected at a resolution of 1.8 Å and 1.85 Å, respectively. The data were processed using *XDS* and scaled using *Aimless*. The *HySS* submodule of the *PHENIX* package (Adams *et al.*, 2010) could locate six selenium atoms and two zinc ions. The structures were refined by *PHENIX* to R_{free} of 20% and 22%, respectively. Figs. 4 and 5 show the anomalous difference maps with superimposed structural models of XPDdr and XPDxc showing the selenium and zinc ion, respectively. The

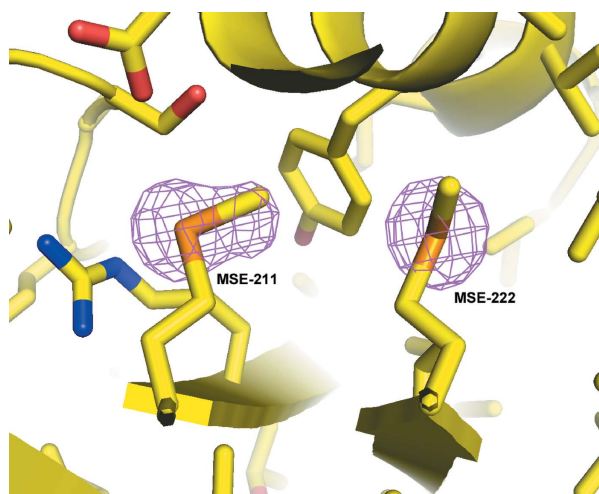


Figure 4
Anomalous difference Fourier map, contoured at 5.0σ and superposed on the structure of XPDdr, near selenomethionine residues (MSE-211 and MSE-222). Illustration by *Pymol*.

structures were validated using Molprobit (Chen *et al.*, 2010) and deposited in the PDB with PDB IDs 5CDE and 5CDL.

6. Conclusions

A protein crystallography beamline, with a biochemistry laboratory in the proximity, has been installed on the bending-magnet port of the 2.5 GeV synchrotron Indus-2. The measured spot size and the photon flux are comparable with the values calculated using the *SHADOW* (Welnak *et al.*, 1994) and *XOP* (Sanchez del Rio & Dejus, 2004) software packages. The measured beam spot size at the sample position is $500\ \mu\text{m} \times 500\ \mu\text{m}$ (FWHM) with reasonably good flux for measurement of diffraction data from crystals of moderate size ($>50\ \mu\text{m}$). The experimental station of PX-BL21 is equipped with a single-axis goniometer, CCD detector ($225\ \text{mm} \times 225\ \text{mm}$), fluorescence detector, cryogenic sample cooler and automated sample changer. This beamline can be used for single-crystal diffraction of macromolecules such as proteins, nucleic acids and their complexes. The X-ray energy in this beamline can be tuned in the range 5–20 keV. Fluorescence scanning equipment is also installed to accurately determine atomic absorption edges and inflection points (Fig. 3). The PX-BL21 beamline is capable of performing anomalous diffraction experiments, as demonstrated by the successful solution of anomalous atom sub-structures for Se and Zn atoms in the case of two new protein crystals.

Since the commissioning of the beamline, a number of users have collected good quality data sets using monochromatic and anomalous diffraction (S-SAD, Se-SAD, Zn-SAD and Mn-SAD). There are about 15 structures deposited in the PDB, many of which are kept on hold. Keeping in mind the number of potential protein crystallographers in India, this number is certain to rise in the coming years. In the future it is planned to upgrade the source from a 1.5 T bending magnet to a superconducting multipole wiggler; ray-tracing calculations

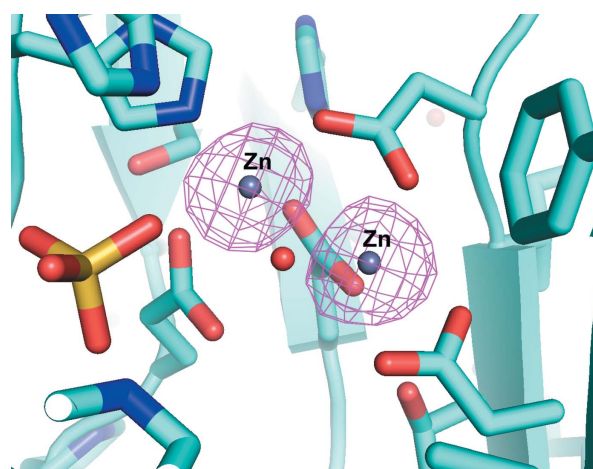


Figure 5
Anomalous difference Fourier map, contoured at 5.0σ and superposed on the structure of the active site of XPDxc, showing two zinc and phosphate ions. Illustration by *Pymol*.

show an improvement of two orders of magnitude in photon flux.

Acknowledgements

The authors are thankful to the front-end and alignment team members of RRCAT for installing the front-end of PX-BL21 and helping in alignment of some of the critical components in the beamline. We would like to place on record and acknowledge the unlimited support extended by Drs P. D. Gupta, S. K. Deb and G. S. Lodha during installation and commissioning. We acknowledge the technical help for protein crystallization by Mr Venkata Are and Ms Pooja Yadav. The authors are also grateful to Dr R. K. Sinha, Chairman AEC, for constant encouragement and to Dr R. Chidambaram for being ever available for advice and discussions.

References

- Adams, P. D., Afonine, P. V., Bunkóczi, G., Chen, V. B., Davis, I. W., Echols, N., Headd, J. J., Hung, L.-W., Kapral, G. J., Grosse-Kunstleve, R. W., McCoy, A. J., Moriarty, N. W., Oeffner, R., Read, R. J., Richardson, D. C., Richardson, J. S., Terwilliger, T. C. & Zwart, P. H. (2010). *Acta Cryst.* **D66**, 213–221.
- Agarwal, S., Biswas, M. & Dasgupta, J. (2015). *Acta Cryst.* **F71**, 401–404.
- Arif, S. M., Geethanandan, K., Mishra, P., Surolia, A., Varshney, U. & Vijayan, M. (2015). *Acta Cryst.* **D71**, 1514–1527.
- Bartels, K. S. & Klein, C. (2003). *The Automar Manual*. Norderstedt: MAR Research GmbH.
- Berman, H., Henrick, K. & Nakamura, H. (2003). *Nat. Struct. Biol.* **10**, 980.
- Chen, V. B., Arendall, W. B., Headd, J. J., Keedy, D. A., Immormino, R. M., Kapral, G. J., Murray, L. W., Richardson, J. S. & Richardson, D. C. (2010). *Acta Cryst.* **D66**, 12–21.
- Ghodke, A. D. & Hannurkar, P. R. (2014). *RRCAT Newsl.* **27**(2), 3.
- Ghodke, A. D., Husain, R., Singh, G. & Indus-2-team (2006). *Beam Dynam. Newsl.* **41**, 77–95.
- Goyal, V. D., Yadav, P., Kumar, A., Ghosh, B. & Makde, R. D. (2014). *Acta Cryst.* **F70**, 1521–1525.
- Hannurkar, P. R. (2015). *RRCAT Newsl.* **28**(1), 3–4.
- Kabsch, W. (2010). *Acta Cryst.* **D66**, 125–132.

- Krolzig, A., Materlik, G., Swars, M. & Zegenhagen, J. (1984). *Nucl. Instrum. Methods Phys. Res.* **219**, 430–434.
- Kumar, A., Are, V. N., Ghosh, B., Agrawal, U., Jamdar, S. N., Makde, R. D. & Sharma, S. M. (2014). *Acta Cryst.* **F70**, 1268–1271.
- Kumar, P., Ghodke, A. D. & Singh, G. (2013). *Pramana J Phys.* **80**, 855–871.
- Leslie, A. & Powell, H. (2007). *Evolving Methods for Macromolecular Crystallography*, edited by R. Read and J. Sussman, Vol. 245, *NATO Science Series*, pp. 41–51. The Netherlands: Springer.
- MacDowell, A. A., Celestre, R. S., Howells, M., McKinney, W., Krupnick, J., Cambie, D., Domning, E. E., Duarte, R. M., Kelez, N., Plate, D. W., Cork, C. W., Earnest, T. N., Dickert, J., Meigs, G., Ralston, C., Holton, J. M., Alber, T., Berger, J. M., Agard, D. A. & Padmore, H. A. (2004). *J. Synchrotron Rad.* **11**, 447–455.
- Pettersen, E. F., Goddard, T. D., Huang, C. C., Couch, G. S., Greenblatt, D. M., Meng, E. C. & Ferrin, T. E. (2004). *J. Comput. Chem.* **25**, 1605–1612.
- Raghuvanshi, V. K., Dhamgaye, V. P., Singh, A. K. & Nandedkar, R. V. (2007). *AIP Conf. Proc.* **879**, 631–634.
- Sanchez del Rio, M. & Dejus, R. J. (2004). *Proc. SPIE*, **5536**, 171–174.
- Schrödinger LLC (2010). *The PyMOL Molecular Graphics System*, Version 1.8. Schrödinger LLC.
- Sheldrick, G. M. (2008). *Acta Cryst.* **A64**, 112–122.
- Sonani, R. R., Sharma, M., Gupta, G. D., Kumar, V. & Madamwar, D. (2015). *Acta Cryst.* **F71**, 998–1004.
- Stewart, D. (1965). *Proc. Inst. Mech. Eng.* **180**, 371–386.
- Welnak, C., Chen, G. & Cerrina, F. (1994). *Nucl. Instrum. Methods Phys. Res. A*, **347**, 344–347.
- Winn, M. D., Ballard, C. C., Cowtan, K. D., Dodson, E. J., Emsley, P., Evans, P. R., Keegan, R. M., Krissinel, E. B., Leslie, A. G. W., McCoy, A., McNicholas, S. J., Murshudov, G. N., Pannu, N. S., Potterton, E. A., Powell, H. R., Read, R. J., Vagin, A. & Wilson, K. S. (2011). *Acta Cryst.* **D67**, 235–242.